July 24, 1964
Project No. 303200
Copy No. 23

STUDY OF THIN FILM LARGE AREA PHOTOVOLTAIC SOLAR ENERGY CONVERTER

Third Quarterly Report
April 1, 1964 - June 30, 1964
Contract No. NAS3-2795

National Aeronautics and Space Administration
Lewis Research Center

Space Power Systems Division

By: Warren J. Deshotels
Frank Augustine

Approved: F. A. Shirland
F. A. Shirland, Head
Solar Battery Section

Hans Jaffe
Hans Jaffe, Director
Electronic Research

Clevite Corporation
Electronic Research Division
Cleveland, Ohio 44108
216 - 851-5500

NASA CR 54145
Project No. 303200

Third Quarterly Report

STUDY OF THIN FILM LARGE AREA PHOTOVOLTAIC SOLAR ENERGY CONVERTER

by

W. J. Deshotels and F. Augustine

Prepared for

NATIONAL AERONAUTICS AND SPACE ADMINISTRATION

July 24, 1964

Contract NAS3-2795

Technical Management
NASA Lewis Research Center
Cleveland, Ohio
Space Power Systems Division
Mr. L. R. Scudder, ME 500-201

Clevite Corporation
Electronic Research Division
Cleveland, Ohio 44108

NOTICE

This report was prepared as an account of Government-sponsored work. Neither the United States nor the National Aeronautics and Space Administration (NASA), nor any person acting on behalf of NASA:

A) Makes any warranty or representation, expressed or implied, with respect to the accuracy, completeness, or usefulness of the information contained in this report, or that the use of any information, apparatus, method, or process disclosed in this report may not infringe privately-owned rights; or

B) Assumes any liabilities with respect to the use of, or for damages resulting from the use of any information, apparatus, method or process disclosed in this report.

As used above, "person acting on behalf of NASA" includes any employee or contractor of NASA, or employee of such contractor, to the extent that such employee or contractor of NASA or employee of such contractor prepares, disseminates, or provides access to any information pursuant to his employment, or contract with NASA, or his employment with such contractor.

Additional copies of this report may be obtained from:

National Aeronautics and Space Administration
Office of Scientific and Technical Information
Washington, D. C. 20546
Attention: AFSS-A

TABLE OF CONTENTS

		Page
NOTICE		i
LIST OF ILLUSTRATIONS		iii
LIST OF TABLES		iv
Section	Title	
	Summary	1
1.	Introduction	1
2.	Evaporated CdS Films	2
	2.1 Evaporator	2
	2.2 Processing Photovoltaic Cells	3
	2.3 Miscellaneous Experiments on Evaporated Films	11
3.	H-Film Substrate Curling Problem	12
4.	Mathematical Models	15
5.	Miscellaneous	22
6.	Work Planned for Next Quarter	22
7.	References	22
8.	Distribution List	23

LIST OF ILLUSTRATIONS

Figure

1. Single Crystal Cell 26 (T5-2). Current-Voltage Characteristics at Increasing Light Intensity. Dashed Line is Dark i-v Curve. Cell Area: 1 cm^2.

2. Single Crystal Cell 28 (T5-4). Current-Voltage Characteristics at Increasing Light Intensity. Dashed Line is Dark i-v Curve. Cell Area: 1 cm^2.

3. Current-Voltage Characteristic for CdS Film Cell 160-4. Cell Area: 7.2 cm^2.

4. Semi-Log Plot of Current-Voltage Characteristic of CdS Film Cell 160-4.

5. Comparison of Theoretical Current-Voltage Characteristic (Solid Curve) and Experimental Current-Voltage Characteristic of CdS Film Cell 160-4. Cell Efficiency = 2.2 Percent.

6. Current-Voltage Characteristics Based on CdS Film Cell 160-4 and ± 10 Percent Variations in i_ν and λ.

LIST OF TABLES

Table		Page
2. 1	Effect of Quartz Cloth Plug on Electrical Properties of Evaporated CdS Films.	4
2. 2	Effect of Changes in Processing on Efficiency of CdS Film Cells.	7
2. 3	CdS Photovoltaic Cells Constructed on H-Film.	8
2. 4	Stability of CdS Evaporated Film Cells.	10

STUDY OF THIN FILM LARGE AREA PHOTOVOLTAIC SOLAR ENERGY CONVERTER

by

Warren J. Deshotels and Frank Augustine
Electronic Research Division, Clevite Corporation

29708

SUMMARY

Sixty one evaporations were completed during this quarter. The evaporator was improved and made more efficient by the addition of heat shields and the elimination of the quartz cloth plug. These changes have resulted in greater uniformity of electrical properties, and better adherence of the film to the substrates. Small but important changes introduced in the fabrication process have resulted in a significant increase in average efficiency from 2.0 to 2.6 percent.

Considerable progress has been made toward solving the curling problem associated with the difference in thermal expansion between CdS and H-Film. Most of the improvement centers around better embossing techniques. Lamination of the cells between sheets of mylar results in flat cells.

A detailed discussion of data analysis is given which shows how well the general equivalent circuit equation represents experimental cells and explains, to some extent, the reasons for the differences that do exist.

Author

1. INTRODUCTION

Present day operational photovoltaic solar energy converters are made of arrays of small silicon cells. Each array may contain hundreds of individual cells interconnected to provide the required level of power. Because silicon is subject to radiation damage, the arrays must be shielded by thin sheets of fused silica. Attempts to reduce the number of individual cells by employing large area silicon cells have so far been unsuccessful although recent advances in growing dendritic, thin, silicon films are promising.

Interest in thin film, large area, cadmium sulfide photovoltaic solar energy converters stems from the fact that such cells have been fabricated with areas as large as thirty-six square inches and conversion efficiencies approaching 3 percent. Furthermore, these films can be put on flexible substrates and are presumed to be highly resistant to radiation damage since they do not depend on high crystalline perfection.

The work described herein is based on the backwall cell arrangement in which sunlight is incident on a highly conducting transparent cadmium sulfide layer and is absorbed in an opaque modified cadmium sulfide layer below the transparent layer. Compared to the frontwall cell, the backwall cell has two principal advantages: 1) The high conductance of the top, transparent, CdS layer minimizes the area of metal grids or bus bars that have to be placed in the path of the incident radiation. 2) The light sensitive layer is protected from the ambient by the relatively thick transparent CdS layer on one side and may be protected by metal foil or another impervious coating on the other.

The principal purpose of this study is the development of a CdS photovoltaic solar energy converter consisting of a large area transparent plastic substrate on which is an array of closely spaced, small (nominally one-inch square), backwall, CdS photocells connected in series or in parallel, depending upon the desired voltage-current output.

2. EVAPORATED CdS FILMS

Sixty one evaporations (Nos. 150 through 205H) were completed during this quarter. The yield was 240 CdS films on 1 inch x 2 inch glass substrates, eight films on 4 inch x 4 inch glass substrates, three CdS films on 4 inch x 4 inch H-Film substrates, ten 3 x 3 arrays of 1 in^2 films on H-Film, one experimental evaporation on a 4 inch x 4 inch sheet of Textolite and three CdS films using nickel screens and H-Film as substrates.

2.1 Evaporator

Tungsten heater coils have been replaced by tantalum coils held in place with fiberfrax. The heat shield reduced heater power requirements

to about 200 watts per heater. The lower heater power results in less spattering -- so much so that the quartz plug was eliminated from all evaporations after No. 159. These changes have resulted in greater uniformity of electrical properties, and better adherence of the film to the substrates. The improvement in the uniformity of electrical properties is chiefly related to elimination of the quartz plug and is demonstrated by the data in Table 2. 1.

Furthermore, the elimination of the quartz plug obviates the necessity of precisely positioning the heater coil around the crucible and leads to a significant time saving.

The decrease in average carrier mobility, noted in the table, does not seem to materially affect film cell quality.

The electrical properties of the evaporated films were nicely reproducible until a new sinter of doped CdS was introduced in May. It was necessary to change the ratio of doped to undoped CdS in order to bring the electrical properties back into the desired range.

2. 2 Processing Photovoltaic Cells

Two important and beneficial changes have been incorporated into the cell fabrication process. One of these is a second application of the slurry to insure complete coverage by the barrier layer; the other is an HCl etch, introduced in June, which increases the short circuit current. Earlier attempts at etching were unsuccessful because of pin holes in the CdS layer and because the layer was not sufficiently adherent to the substrate. With the present evaporation techniques, the number of pin holes is greatly reduced and adherence is improved enough to withstand removal of the "scotch tape" employed in masking. The fabrication process in use at the end of this quarter is:

1. Wash thoroughly with acetone.
2. Apply "scotch tape" mask for n-type electrode.
3. Electroplate nickel n-type electrode.
4. Wash in distilled H_2O and remove masking tape.
5. Wash thoroughly in acetone.
6. Dry with jet of argon gas.

Table 2.1 Effect of Quartz Cloth Plug on Electrical Properties of Evaporated CdS Films.

	Evaporation No.	Thickness, cm x 10^{-3}	Resistivity, ohm-cm	Carrier Concentration, cm^{-3} x 10^{-18}	Carrier Mobility, $cm^2 volt^{-1} sec^{-1}$
Evaporation With Quartz Plug	150	4.3	0.046	6.7	20
	151	5.7	0.034	6.8	28
	152	5.1	0.050	6.3	20
	153	4.1	0.021	8.7	34
	154	4.8	0.012	8.7	58
	155	3.4	0.020	7.8	40
	156	5.5	0.011	8.6	69
	157	2.7	0.180	3.5	10
	158	3.5	0.056	6.2	18
	159	3.6	0.050	8.2	16
Average		4.3 ± 0.8	0.048 ± 0.029	7.2 ± 1.3	31 ± 15
Evaporation Without Quartz Plug	160	4.0	0.100	5.7	11
	161	3.7	0.087	6.5	11
	162	4.0	0.079	6.6	12
	164	4.6	0.082	6.3	12
	166	4.4	0.076	6.3	13
	167	3.6	0.090	6.9	10
	170	4.7	0.070	6.7	13
Average		4.1 ± 0.3	0.083 ± 0.008	6.4 ± 0.3	12 ± 1

7. Etch CdS film for 20 to 30 seconds in solution of 3 parts conc. HCl and 1 part distilled H_2O.

8. Rinse thoroughly and dry with jet of argon gas. Surface of CdS should have matte appearance similar to that of c-minus face of etched single crystal CdS.

9. Heat film to 80°C.

10. Brush slurry onto heated film and dry at 80°C.

11. Brush off excess slurry and rinse and brush thoroughly with jet of distilled H_2O.

12. Dry film with argon jet.

13. Repeat slurry application on cold film and dry.

14. Heat in 250°C oven for 2 minutes.

15. Quench and remove excess slurry with brush and argon jet.

16. Heat in 250°C oven for 3 minutes and quench.

17. Apply barrier electrode of air drying silver paint. Reinforce nickel n-type electrode with silver paint.

18. Dry paint completely.

19. Heat in 250°C oven for 5 minutes.

20. Quench, obtain i-V characteristic.

21. Repeat steps 19 and 20 if necessary.

A steady improvement in the quality of CdS film cells has been observed during this quarter. In April, a group of eleven cells, fabricated according to the process given in the Second Quarterly Report,[1] had efficiencies ranging up to 1.6 percent. A second group of twenty cells, fabricated in the same manner but given a second slurry application had efficiencies ranging from 1.7 to 2.6 percent and averaging 2.2 percent. In May, a group of 19 cells, fabricated with the double slurry application, also averaged 2.0 percent efficiency with the range increased to 0.8 to 3.0 percent.

In May, etching with dilute HCl was added to the present process. Fifteen cells averaged 2. 0 percent efficiency with a range of 0. 9 to 2. 9 percent. In June the etchant was made more concentrated resulting in the fabrication procedure given in this section. Eleven cells fabricated according to this latest process averaged 2. 6 percent efficiency with a range of 1. 8 to 3. 1 percent. In addition, large area cells of high efficiency were fabricated for the first time. These cells had areas of 70. 0, 73. 3 and 75. 2 cm^2 respectively and efficiencies of 2. 1, 2. 8, and 3. 0 percent respectively. These data are summarized in Table 2. 2.

Two of the evaporations on H-Film were not processed because the CdS was not adherent. One of these was a large area (3 inch x 3 inch) CdS layer on lapped but unembossed H-Film. The other was also a large area CdS layer on a piece of H-Film that was cold embossed with a wire screen. The screen pattern faded when the substrate was heated during the evaporation. In both cases, it appeared that the H-Film had not been completely cleaned after lapping.

Three other CdS arrays on H-Film were processed in experiments to determine the best n-electrode material and electrode configuration. It was pointed out in the Second Quarterly Report that nickel and gold seemed to be the best available metals for electroding CdS films with nickel making a somewhat better contact than gold. Indeed, electroplated nickel is used almost exclusively for glass backed cells. Electroplated nickel cannot generally be applied to CdS on embossed H-Film because of the masking problems presented by the embossed pattern. It is, therefore, more feasible to evaporate the n-electrode on H-Film cells. Nickel is difficult to evaporate, while evaporating gold is quite easy. The three arrays on H-Film were to compare evaporated nickel vs evaporated gold as electrode material. It is seen in Table 2. 3 that there seems to be no significant advantage of one metal over the other.

In array 178H, the two cells, 178H-c and 178H-i showed very high series resistance in the forward direction. This is not uncommon with evaporated gold electrodes, and is usually denoted by a sharp break in the forward characteristic as the curve crosses the horizontal (voltage) axis. The slope of the curve in the first quadrant may change

Table 2.2 Effect of Changes in Processing on Efficiency of CdS Film Cells.

Cell No.	V_{oc}, volts	i_{sc}, mA	Area, cm^2	Fill Factor	Efficiency %	Notes
170-3	0.38	44.0	4.6	0.52	1.9	
170-4	0.35	54.5	5.5	0.56	1.9	
170-7	0.40	42.0	5.0	0.66	2.2	
171-1	0.40	66.0	7.0	0.49	1.9	
171-3	0.35	22.0	4.6	0.42	0.8	
171-7	0.39	67.0	7.3	0.53	1.9	Fabricated according to process described in Second Quarterly Report except for second slurry application.
172-4	0.40	63.0	6.6	0.38	1.4	
173-5	0.39	68.0	6.9	0.60	2.3	
174-2	0.39	50.7	6.6	0.60	1.8	
174-3	0.40	58.6	6.9	0.63	2.1	
174-4	0.40	51.7	5.4	0.59	2.3	
175-1	0.41	67.0	6.0	0.63	2.9	
175-2	0.41	49.0	5.5	0.60	2.2	
175-3	0.41	64.0	4.8	0.54	3.0	
181-3	0.41	52.0	6.6	0.63	2.0	
181-7	0.37	54.0	7.0	0.62	1.8	
184-4	0.41	75.0	8.3	0.54	2.0	
185-3	0.37	41.0	6.2	0.46	1.2	
186-4	0.44	72.0	7.2	0.59	2.6	
Average					2.0 ± 0.4	
184-1	0.38	72.0	8.2	0.49	1.7	
184-6	0.40	97.0	8.5	0.51	2.3	
185-4	0.35	78.0	8.3	0.53	1.7	
187-5	0.40	15.5	3.5	0.48	0.9	
188-3	0.42	91.0	8.4	0.44	2.0	
188-4	0.44	46.5	4.5	0.46	2.1	
188-5	0.42	56.5	7.1	0.36	1.2	Fabricated as above with addition of weak HCl etch.
188-6A	0.42	25.0	2.9	0.59	2.2	
188-6B	0.40	24.5	2.5	0.56	2.1	
188-7	0.42	54.5	4.8	0.30	1.8	
189-3	0.39	94.0	8.1	0.57	2.6	
189-4	0.41	100.0	7.9	0.57	2.9	
189-6	0.38	110.0	8.6	0.55	2.7	
190-5	0.35	84.0	8.1	0.50	1.8	
190-6	0.41	92.0	8.3	0.53	2.4	
Average					2.0 ± 0.4	
55-4	0.36	86.0	7.5	0.60	2.5	
117-2	0.41	27.3	3.0	0.48	1.8	
184-5	0.40	112.0	7.8	0.54	3.1	
185-1	0.38	51.5	4.9	0.55	2.2	Fabricated according to process described in this report with more concentrated etch.
189-5	0.39	95.0	8.2	0.52	2.5	
189-8	0.41	107.0	7.5	0.52	3.0	
190-4	0.39	118.0	7.9	0.51	3.0	
190-8	0.41	104.0	7.6	0.46	2.6	
200-1	0.41	820.0	70.0	0.43	2.1	
201-1	0.38	1070.0	73.3	0.51	2.8	
202-1	0.42	1000.0	75.2	0.50	3.0	
Average					2.6 ± 0.3	

Table 2.3 CdS Photovoltaic Cells Constructed on H-Film

Cell No.	V_{oc}, volts	i_{sc}, mA	Area, cm^2	Fill Factor	Efficiency %	Slurry
178Ha	.38	26.2	3.0	.48	1.7	S-33
178Hb	.38	27.2	3.1	.57	1.9	S-33
178Hc	.38	26.4	2.9	.42	1.5*	S-33
178Hd	.37	21.5	2.6	.56	1.7	S-33
178He	.37	24.2	2.3	.48	1.9	S-33
178Hf	.37	23.3	2.2	.49	1.9	S-33
178Hg	.37	27.4	2.6	.50	2.0	S-33
178Hh	.36	26.8	2.6	.50	1.9	S-33
178Hi	.35	22.3	2.6	.47	1.4*	S-33
Average					1.8 ± 0.2	

*High series resistance in forward direction. Evap. Au n-electrodes.

180Ha*	.42	23.7	2.6	.50	1.9	S-33
180Hb	.39	28.6	2.6	.42	1.8	S-33
180Hc	.38	23.0	2.6	.45	1.6	S-33
180Hd	.40	29.6	2.6	.47	2.0	S-33
180He	.40	27.8	2.6	.42	1.8	S-33
180Hf	.38	21.4	2.6	.41	1.4	S-33
180Hg	.37	26.6	2.6	.43	1.6	S-33
180Hh	.34	25.6	2.6	.40	1.3	S-33
180Hi	.37	17.7	2.6	.40	1.0	S-33
Average					1.6 ± 0.2	

*Evaporated Au n-electrodes.

183Ha*	.43	20.8	2.6	.54	1.9	S-33
183Hb	.43	17.4	2.6	.53	1.6	S-33
183Hc	.44	14.0	2.6	.55	1.3	S-33
183Hd	.42	16.2	2.6	.52	1.4	S-33
183He	.41	21.4	2.6	.48	1.6	S-33
183Hf	.42	17.0	2.6	.54	1.5	S-33
183Hg	.41	18.0	2.6	.61	1.7	S-33
183Hh	.41	16.8	2.6	.42	1.0	S-33
183Hi	.42	16.7	2.6	.54	1.5	S-33
Average					1.5 ± 0.2	

*Evaporated Ni n-electrodes.

by an order of magnitude from that in the fourth quadrant. The sharp break in the characteristic usually disappears if the contact is heated, but the overall resistance of the cell remains high.

The sharp break is not as noticeable in array 180H and is not present at all in array 183H, the latter having evaporated nickel electrodes.

Another large area H-Film cell, No. 193H, was fabricated before the introduction of the etch step in the fabrication process. Its area was 63 cm^2 and its efficiency was 1.0 percent. It is expected that the etch will improve the efficiency considerably, and an experiment is in progress to attempt to verify this.

Attempts have been made to put an evaporated metal grid on H-Film to act as a current collector from the CdS. Gold has been found to adhere reasonably well to H-Film, so in these preliminary experiments, gold grids were evaporated and then built up by electroplating nickel onto the gold. The grid consists of 1/16 inch wide stripes located on 1/2 inch centers, stretching across the H-Film from one edge to the other. The stripes are connected together through a single transverse stripe, 1/8 inch wide, crossing the grid at its center. In the first attempt, the grid was partly removed while being cleaned prior to the CdS evaporation. A second grid was prepared and extreme care exercised to keep the grid and H-Film clean so that only a distilled water rinse was required prior to evaporation. The evaporated layer of CdS pulled the grid free of the H-Film. Additional experiments along these lines will be carried out. A similar attempt on a glass substrate was unsuccessful when the barrier layer shorted out to the grid through pinholes in the CdS layer.

Five cells, fabricated in April, were examined for stability after a few days storage in either a dry box or vacuum desiccator. The data are given in Table 2.4.

In all but one instance the cells recovered their original efficiency after absorbed mositure was removed by the additional heating. Cell 120-1 was apparently damaged by the additional heating. No long term

Table 2.4 Stability of CdS Evaporated Film Cells

Cell No.	Date of Fabrication	Efficiency at Fabrication	No. of Days in Storage	Efficiency After Storage	Additional Heating	Efficiency After Heating
98-1	4/24/64	1.8%	6 (dry box)	1.8%	2 min @ 250°C	1.8%
120-1	4/30/64	1.5%	1 (desiccator)	1.4%	5 min @ 250°C	1.3%
156-4	4/27/64	2.4%	5 (dry box)	1.8%	2 min @ 250°C	2.4%
167-3	4/27/64	2.3%	5 (dry box)	2.0%	1.5 min @ 250°C	2.3%
170-6	4/30/64	1.9%	2 (desiccator)	1.6%	2 min @ 250°C	1.9%

permanent deterioration has been observed so far. It is tentatively concluded that the observed deterioration is due to water vapor.

2.3 Miscellaneous Experiments on Evaporated Films

Experiments were performed involving electroformed gold or nickel mesh having 70 lines per inch. In one experiment, gold mesh was pressed into H-Film at 230°C and 20,000 lbs force. The mesh and H-Film were each 3 inch x 3 inch squares. The mesh appeared well embedded in the 2 mil thick H-Film. The H-Film was clamped between two sheets of glass, each containing a 2.5 inch diameter hole, and CdS was evaporated thereon. The idea behind this experiment was, of course, to use the mesh as a transparent electrode to the n-type CdS. The completed film withstood processing but yielded a very low efficiency cell. However, the feasibility of such a cell was demonstrated.

In another experiment, an attempt was made to construct an evaporated layer on H-Film with a mesh screen for the n-type electrode. In this case, however, the mesh was not pressed into the H-Film, but simply imbedded in the CdS layer. The evaporated layer structure was successful but incomplete and the barrier shorted out during processing. In another experiment a layer of CdS was deposited on a mesh as sole substrate. Except for a few places where the CdS did not fill in completely, the evaporated film looked quite good. However, during the fabrication process, etching destroyed the film.

All of these experiments were conducted with the two glass plates mentioned above used as clamps for the mesh or H-Film and mesh combinations.

A sample of Textolite, manufactured by the General Electric Co., was obtained. This particular material is a glass fiber filled silicone resin. Its thermal and electrical stability appear to be as good as those of H-Film. The Textolite has successfully withstood temperatures of 250°C for several hours with no visible effects. A sheet 0.008 inches thick is water white in color, and transmits about 75 percent of the light from a photoflood lamp as determined with a silicon standard photovoltaic cell compared with about 82 percent transmission by H-Film.

This difference is probably due to scattering by the glass fibers. True spectral transmission will be examined later. Information concerning the physical characteristics of Textolite has been requested. The chief interest in this material lies in the fact that Textolite is thermoplastic and is self bonding to metals. Some of the uncured material has been requested. If obtained, an attempt will be made to bond a piece of electroformed nickel mesh and a CdS cell made therefrom. A layer of CdS was deposited on the Textolite sheet but did not adhere. Other experiments will be carried out when additional supplied of Textolite are obtained.

3. H-FILM SUBSTRATE CURLING PROBLEM

A number of experiments were performed in which H-Film substrates were embossed in various ways. Two of the usual 3 x 3 CdS arrays were deposited on unembossed H-Film to determine the armount of curling and the sites at which curling was most severe. One array was deposited on the convex side of an H-Film substrate embossed with 1/8 inch diameter hemispheres. The CdS adhered very poorly and curling was unusually severe, especially around the holes made by the clamping screws, confirming anticipated results. In two other experiments a wire screen was used for the embossing die. The first film was cold pressed on the screen with a force of 20,000 lbs (1250 psi); the second was hot pressed at 100°C and 10,000 lbs (650 psi). The wire screen is a neutral optical filter of about 50% transmission. In both cases, the embossed H-Film curled strongly along the grain of the screen. In another experiment the H-Film was pressed on the screen, rotated 90°, and pressed again. The film tended to curve hemispherically and in such a direction as to oppose the curling expected from the CdS. An evaporated CdS layer deposited on this film curled the H-Film in the usual manner, however the radius of curvature, about 2 inches, was not as small as observed in previous experiments.

Evaporation No. 203H was made using a lapped, 2 mil thick piece of H-Film which had been heated to 100°C and pressed at 30,000 lbs

for 1 minute. The die was a screen having 45 percent optical transmission. A 3 x 3 array of 1 in^2 CdS layers was evaporated onto the H-Film and on cooling to room temperature curled into a cylinder about 1 inch in diameter. This film was reverse-wound on a 1 inch diameter mandrel and heated to 250°C for 1 hour. When cooled and released it curled as before. Therefore, annealing is not the solution.

Another experiment repeated the above except that the embossing took place at 234°C and 30,000 lbs force. CdS was again deposited in a 3 x 3 array, and on cooling the sheet curled into a half cylinder about 2 inches in diameter. This demonstrated that high embossing temperatures and pressures were desirable.

In evaporation No. 205H, the H Film substrate was only 1 mil thick. The substrate was lapped but not embossed, and a large area (3 inch x 3 inch) CdS layer was evaporated. The film lay flat with only slight bowing when taken from the vacuum chamber. Adherence was poor and the CdS layer cracked badly when the film was flexed. This experiment indicates that very thin H-Film substrates may yield enough on cooling that curling will be eliminated. Additional experiments will be carried out as soon as more of the 1 mil and 1/2 mil H-Film can be obtained.

It was suggested that some of the curling might be due to stress-relief in H-Film during evaporation. An attempt to stress-relieve H-Film before evaporation was made. A sheet of 2 mil thick H-Film was placed between two sheets of aluminum and heated at 250°C for thirty minutes. No noticeable change was observed on cooling and no decrease in curling was observed after evaporation. Thus it appears that stress-relief is not a significant problem.

A five mil thick sheet of H-Film was also tried in order to see if strengthening the substrate would prevent curling after evaporation. The H-Film was heated to 250°C and while hot, was pressed at 30,000 lbs for one minute with the screen. After evaporating a 3 x 3 CdS array, the film curved into an open half cylinder about 2.5 inch in diameter. Adherence was very good. One of the 1 in^2 sections was cut out and

fabricated into a photovoltaic cell. Somewhat greater curling was observed after processing.

This experiment was repeated using a three mil thick sheet of H-Film. Essentially identical results were obtained.

A jig was constructed to hold steel bearing balls in a close packed hexagonal array. It was filled with 0. 125 inch diameter balls and used to emboss a 2 mil thick piece of H-Film. The temperature of the system was raised to 240°C and then a force of 10, 000 lbs was exerted. After one minute the force was released and the H-Film was removed and allowed to cool. The embossed substrate was limp and lay flat. After evaporating CdS the radius of curvature was about 1. 8 inch. When a 3 x 3 array was deposited the radius of curvature increased slightly. This is by far the best embossed film obtained thus far.

Some of the embossed substrates have been pressed between sheets of mylar and nylon after evaporation. These packages do not exhibit any significant curvature. Completely electroded dummy cells have been packaged in this manner with excellent results. This is not the most desirable configuration, however, and the following experiments are planned for the immediate future:

1. Continuation of the embossing experiments with 0. 125 inch and 0. 063 inch diameter balls.

2. Continuation of the mylar encapsulation of embossed and unembossed films with particular attention to working cells.

3. Encapsulation of embossed and unembossed films with teflon coated H-Film. This has the principal advantage of involving only one additional sheet of plastic contrasted to the two or more sheets required with mylar encapsulation; and the additional advantage of having only H-Film in the sun side of the package. This may be successful only with the 3 x 3 arrays since teflon probably does not adhere well to the barrier electrode but should adhere well to the bare H-Film strips between the cells in the 3 x 3 array.

4. MATHEMATICAL MODELS

The mathematical analysis of film cell data and of the idealized model of a photovoltaic cell continues to be very interesting. As pointed out in previous reports the most general equivalent circuit consists of a constant current generator shunted by an ideal diode and a fixed internal shunt resistance, all in series with a fixed series internal resistance. The equation for this model is

$$i = i_{\nu} - i_{o}(e^{\lambda(V-iR_s)} - 1) + \frac{V-iR_s}{R_{sh}} , \qquad (4-1)$$

where i and V are respectively the current and voltage measured at the cell terminals, i_{ν} is the light generated current, i_o is the reverse saturation current, R_s and R_{sh} are respectively the internal series and shunt resistances, and $\lambda = -q/AKT$ is a parameter involving the carrier charge, q, the Boltzman constant, K, the absolute temperature, T, and a parameter, A, which depends on the kind of rectifying barrier present in the diode.

For a p-n junction with diffusion limited currents, $A=1$; for a junction with recombination current limitations, $A=2$ or more. Shockley[2] developed the diffusion theory of the photovoltaic effect in p-n junctions in germanium which led to $A=1$. Sah, Noyce and Shockley,[3] developed the recombination current theory for silicon solar cells and showed how recombination currents led to $A=2$. Queisser[4] showed how larger values of A could be obtained for silicon (in agreement with experimental evidence) based on "pipes" and dislocations.

In the case of cadmium sulfide photovoltaic cells, values of A as large as 15 have been reported and it has frequently been stated that A must be between 3 and 5 for good CdS cells. Grimmeiss and Memming[5] were the first (and perhaps the only) workers in this field to claim that CdS treated with copper produced a true p-n junction with a measured $A = 1.1$.

The measurements made on CdS photovoltaic cells in this laboratory, while not definitive, do show interesting correlations with the

results of computer solutions of Eq. (4-1). For example, the computer curves show that if the series resistance, R_s, is increased (while holding all other parameters constant) the forward characteristic is rotated clockwise about the open circuit voltage point; the short circuit current point remains unchanged and consequently the family of curves merges into a single line in the third quadrant whose slope, dV/di, is the sum of shunt and series resistance of the cell. This sort of behavior is exhibited in Fig. 1 which shows the current-voltage characteristics of a single crystal CdS photovoltaic cell for increasing light intensity. Notice, however, that the point of rotation of the forward characteristics is actually above the voltage axis. This is due to the fact that the open circuit voltage depends on the incident light intensity and therefore Fig. 1 shows the combination of two effects: the rotation of the forward characteristics and the horizontal displacement of the open circuit voltage. Thus, one may conclude that the series resistance is light dependent. This is also demonstrated by the fact that the dark characteristics (dashed line) is displaced well to the right of the family of light characteristics and dV/di for this curve is much larger than dV/di for any of the light characteristics. Notice also the parallelism of the curves in the third quadrant; for although the curves necessarily do not have a common short circuit current ($i_{sc} = i_\nu$ is proportional to light intensity) the third quadrant slopes, dV/di, are all about equal.

It must be pointed out here that dV/di, measured in the first quadrant, is related to the series resistance, R_s, but is not itself the series resistance, i. e., $dV/di \neq R_s$; but dV/di, measured in the third quadrant, is very nearly the shunt resistance, R_{sh}. This will be discussed in some detail later.

As another example of the correlation between experimental and computer curves, the latter show that if the shunt resistance, R_{sh}, is decreased (while holding all other parameters constant) the open circuit voltage point is displaced to smaller values, i. e., to the left. At the same time, the slopes of the forward characteristics are unchanged while the slopes in the third quadrant do change since $dV/di \cong R_{sh}$ here.

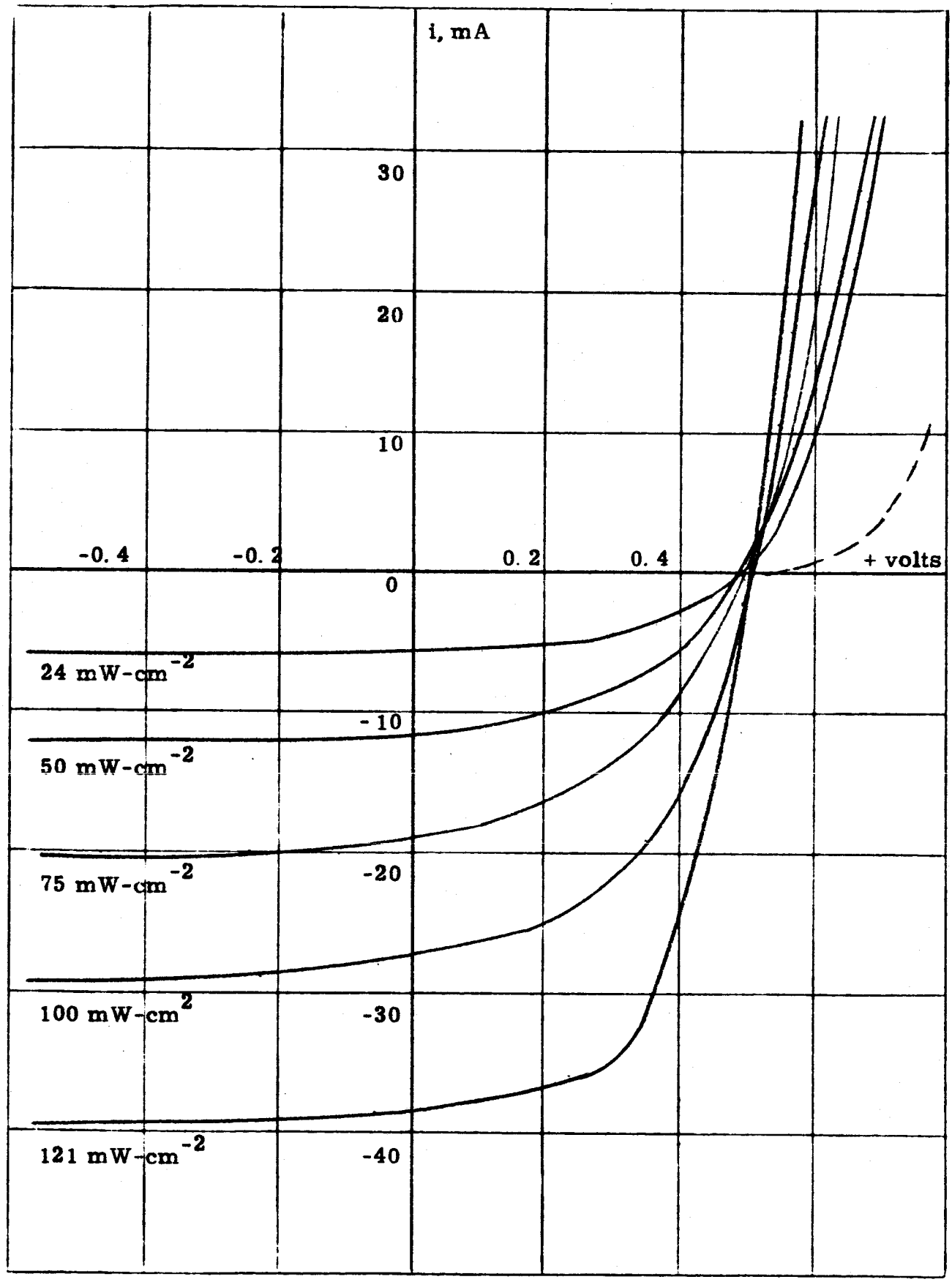

FIG. 1. SINGLE CRYSTAL CELL 26(T5-2). CURRENT-VOLTAGE CHARACTERISTICS AT INCREASING LIGHT INTENSITY. DASHED LINE IS DARK i-v CURVE. CELL AREA: 1 cm^2

This sort of behavior is shown in Fig. 2 which shows the current voltage characteristics of another single crystal CdS photovoltaic cell for increasing light intensity. In this case, of course, it is impossible to distinguish between the two causes of V_{oc} displacement: the shift due to the change in light intensity or to the change in R_{sh}. On the other hand, dV/di for the curves in the third quandrant does, in general, decrease as the light intensity increases. This means, of course, that the shunt resistance is light dependent.

As yet there is no satisfactory way of introducing the light dependent series and shunt resistances into the equivalent circuit equation. A considerable effort involving a great many measurements of R_s and R_{sh} at different light intensities would be required in order to characterize the light dependence mathematically.

Earlier, it was mentioned that $dV/di \neq R_s$ in the first quadrant while $dV/di \cong R_{sh}$ in the third quadrant. This is easily verified by differentiating Eq. (4-1), obtaining an expression for di/dV, and inverting. The manipulations are straightforward and the result is

$$\frac{dV}{di} = R_s + \left[\frac{1}{R_{sh}} - i_o \lambda e^{\lambda(V - iR_s)}\right]^{-1} . \qquad (4\text{-}2)$$

This is a general expression which becomes more useful when evaluated at certain points, namely at the points, $i=0$, $V=V_{oc}$; $i=i_{sc}=i_{\nu}$, $V=0$; and in the third quadrant where both V and i are negative.

At the point $i=0$, $V=V_{oc}$,

$$\left.\frac{dV}{di}\right|_{i=0} = R_s + \left[\frac{1}{R_{sh}} - i_o \lambda e^{\lambda V_{oc}}\right]^{-1} , \qquad (4\text{-}3)$$

at the second point,

$$\left.\frac{dV}{di}\right|_{V=0} = R_s + \left[\frac{1}{R_{sh}} - i_o \lambda e^{-\lambda i R_s}\right]^{-1} . \qquad (4\text{-}4)$$

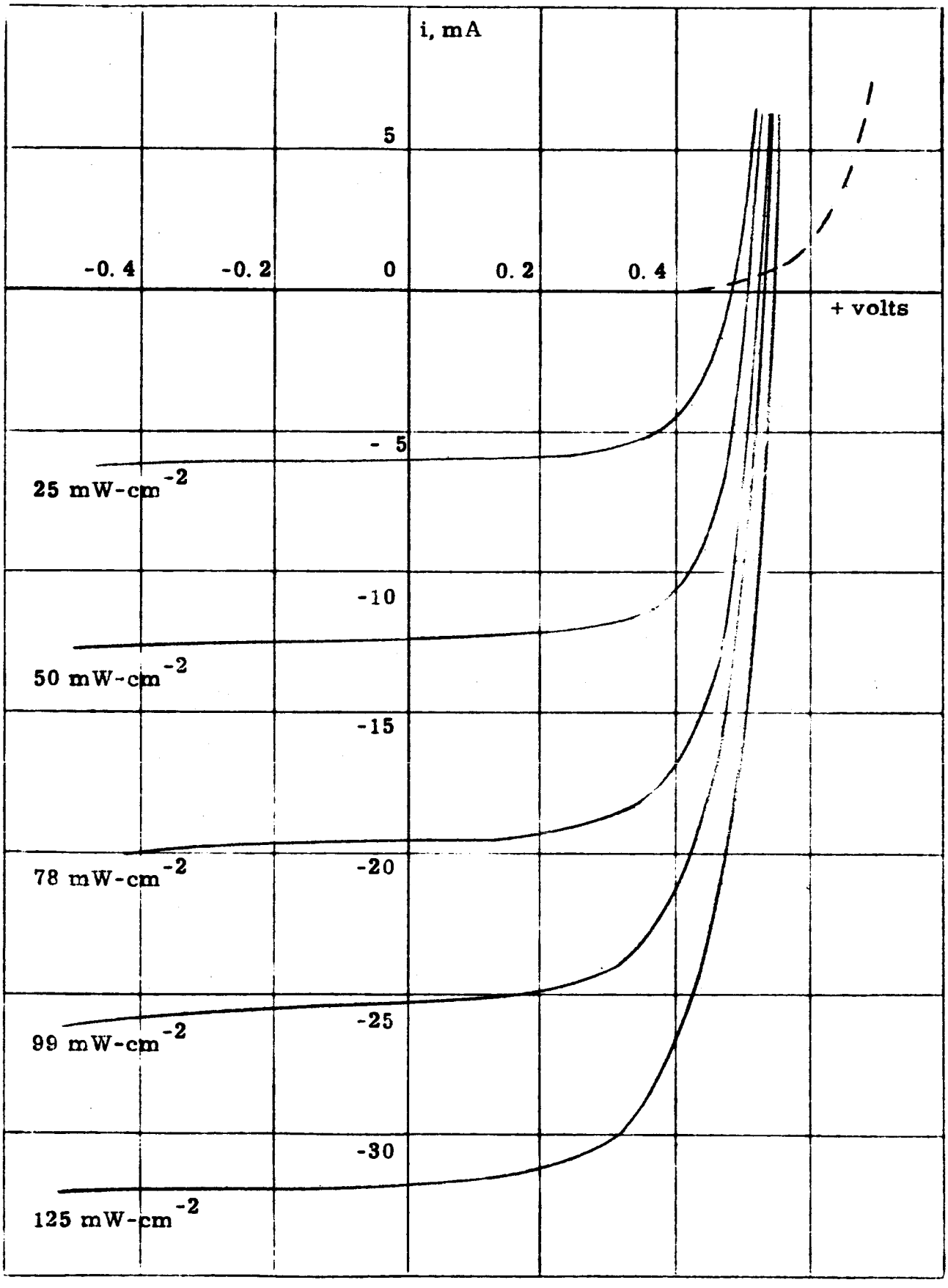

FIG. 2. SINGLE CRYSTAL CELL 28 (T5-4). CURRENT-VOLTAGE CHARACTERISTICS AT INCREASING LIGHT INTENSITY. DASHED LINE IS DARK i-v CURVE. CELL AREA: 1 cm^2

Before evaluating dV/di in the third quadrant, it is well to point out that Eq. (4-3) illustrates the fact that the slope of the forward characteristic does not represent the series resistance. In fact, it is possible to replace i_o in Eq. (4-3) by its equivalent obtained from Eq. (4-1) by setting $i=0$, $V=V_{oc}$, which is

$$i_o = \frac{i + V_{oc}/R_{sh}}{e^{\lambda V_{oc}} - 1} \quad . \tag{4-5}$$

Substituting into Eq. (4-3), one obtains

$$\left.\frac{dV}{di}\right|_{i=0} + R_s + \left\{ \frac{1}{R_{sh}} - \frac{\left[i_\nu + V_{oc}/R_{sh}\right]}{\left[e^{\lambda V_{oc}} - 1\right]} \left[\lambda e^{\lambda V_{oc}}\right] \right\}^{-1} . \tag{4-6}$$

For most of the CdS photovoltaic cells encountered today, $e^{\lambda V_{oc}} >> 1$, and Eq. (4-6) may be reduced to

$$\left.\frac{dV}{di}\right|_{i=0} + R_s + \left\{ \frac{1}{R_{sh}} - \left[i_\nu + V_{oc}/R_{sh}\right] \lambda \right\}^{-1} . \tag{4-7}$$

This may be rearranged to give

$$\left.\frac{dV}{di}\right|_{i=0} + R_s + R_{sh} \left[1 - \lambda e_\nu R_{sh} - \lambda V_{oc}\right]^{-1} . \tag{4-8}$$

It is not possible to express each factor in terms of some measured or even theoretically known value, but it is possible to obtain an order of magnitude approximation for the second term on the right of Eq. (4-8). For a fairly typical CdS cell, dV/di is of the order 1, V_{oc} is of the order of 0.5 volt, λ is of the order of 20 V^{-1}, i_ν is of the order of -0.1 amp for a cell area of 10 cm^2, and R_{sh} is of the order of 200 ohms. Substituting these into Eq. (4-8),

$$\left.\frac{dV}{di}\right|_{i=0} = 1 = R_s + \left[1-(20)(-0.1)(200) - (20)(0.5)\right]^{-1} ,$$

$$\left.\frac{dV}{di}\right|_{i=0} = 1 = R_s + \frac{200}{391} ,$$

$$\left.\frac{dV}{di}\right|_{i=0} = 1 = R_s + \frac{1}{2} .$$

Thus, R_s is also of the order of the term involving R_{sh}, and a significant error is introduced if this is not taken into account. Obviously, for very efficient cells, even of large area, the correction becomes smaller, but is not negligible until efficiencies greater than about 5 percent are reached while shunt resistances in excess of about 100 ohms are maintained.

Returning, now, to the evaluation of Eq. (4-2) in the third quadrant, it is convenient to clear the fraction on the right side and obtain

$$\left.\frac{dV}{di}\right|_{V<0} = R_s + R_{sh}\left[1-i_o\lambda R_{sh}\, e^{\lambda(V-iR_s)}\right] . \qquad (4\text{-}9)$$

In the third quadrant, V and i are both negative, and for values of V such that $|V| - |iR_s|$ is small (i.e., for V equal to a few tenths of a volt) the term $i_o\lambda R_{sh}\, e^{\lambda(V-iR_s)}$ is generally negligible compared to unity except in the case where i_o is very large. For typical CdS cells, i_o is usually small so that Eq. (4-9) reduces to

$$\left.\frac{dV}{di}\right|_{V<0} = R_s + R_{sh} . \qquad (4\text{-}10)$$

Usually, $R_s << R_{sh}$ and so the slope of the curve in the third quadrant is a good approximation to R_{sh}.

The only other parameter in Eq. (4-1) not discussed so far is λ. There is no satisfactory way of obtaining λ from experimental i-V characteristics, even when the data are replotted on semi-log graph paper. The reason for this is obvious when one remembers that

experimentally, only the terminal current and voltage are obtained from a CdS cell, and a semi-log plot would yield a straight line only if i and V were related by an equation of the type

$$i = ae^{\lambda V} + b \quad , \tag{4-11}$$

instead of the type which is Eq. (4-1). In general, when the experimental i , V values are plotted on semi-log paper, an S shaped curve is obtained and only good judgment (or guessing) permits one to obtain a reasonable value for λ which when substituted into Eq. (4-1) yields good agreement between the theoretical and experimental curves.

As a typical example, Fig. 3 shows the experimental data for CdS film cell 160-4. This happens to be a glass backed cell made in this laboratory in April. Its area is 7.2 cm^2 but its efficiency is only 2.2 percent and therefore embodies all of the difficult aspects of the type of analysis being described.

When these data are replotted on semi-log paper, one obtains the curve of Fig. 4. Here, of course, it is necessary to plot $i-i_\nu$ in order to avoid negative numbers. The slope of the curve between the arrows was chosen for the evaluation of λ. The value obtained was 13.42 V^{-1}. The lower portion of the curve yields 9.15 V^{-1} for the value of λ and a least squares fit of all points to a straight line yields a value of 10.9 V^{-1}. However, it will be pointed out later that even the value 13.42 V^{-1} is too small.

In order to test the suitability of Eq. (4-1) for describing CdS photovoltaic cells, it is necessary also to obtain values for R_s, R_{sh} and i_o. The short circuit current, i_ν, and V_{oc} are determined directly from Fig. 3. It has already been pointed out that R_{sh} may be determined directly from the i-V characteristic. Figure 3 gives a value of 180 ohms for R_{sh}. The series resistance, R_s, and i_o may be determined from Eqs. (4-3) and (4-5), even though the validity of R_s determined in this manner is questionable. For the present case, R_s was 0.033 ohms; $i_o = -1.864 \times 10^{-4}$ A. These numbers were substituted into Eq. (4-1) and a table of i vs V tabulated by

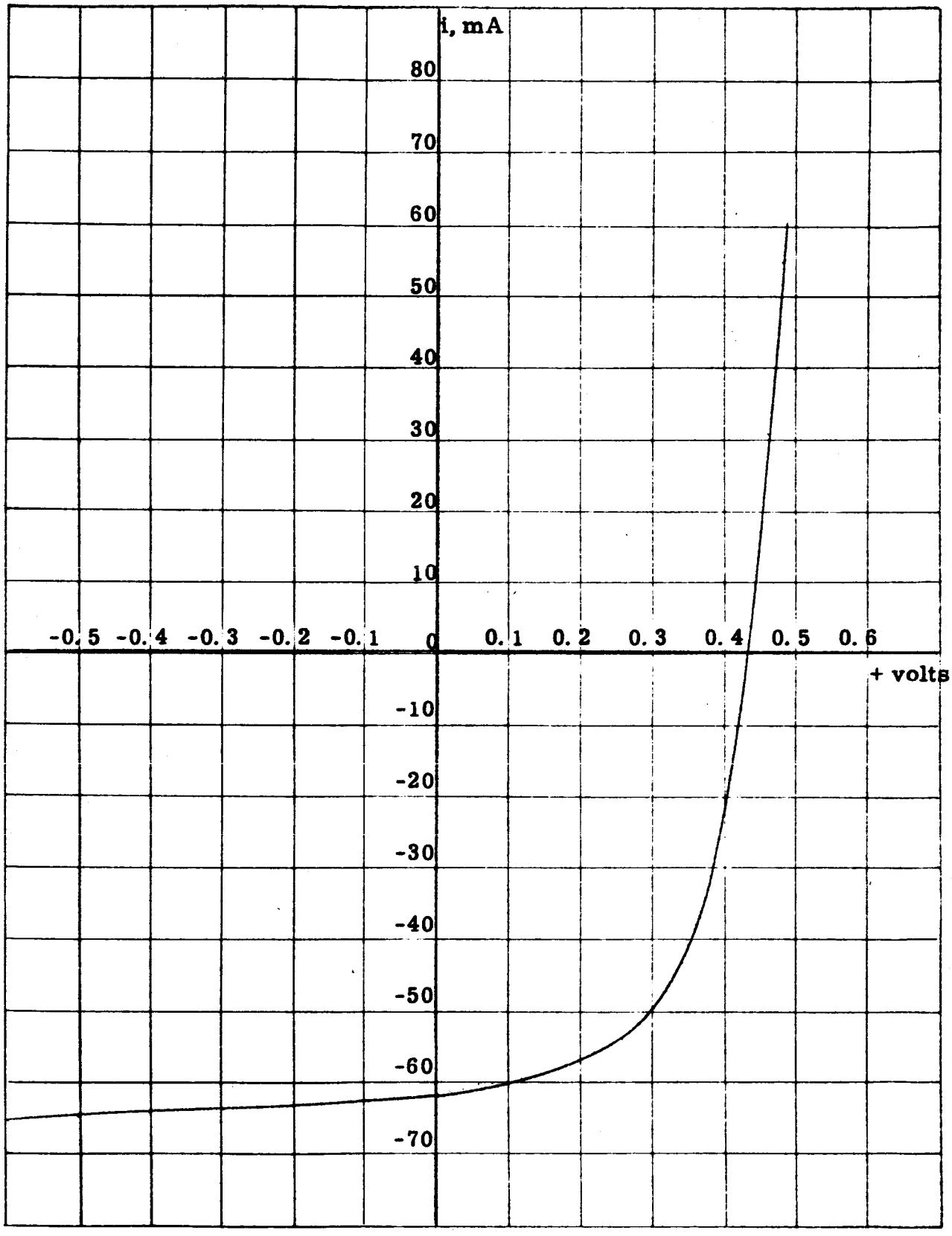

FIG. 3 CURRENT-VOLTAGE CHARACTERISTIC FOR CdS FILM CELL 160-4. CELL AREA: 7.2 cm^2

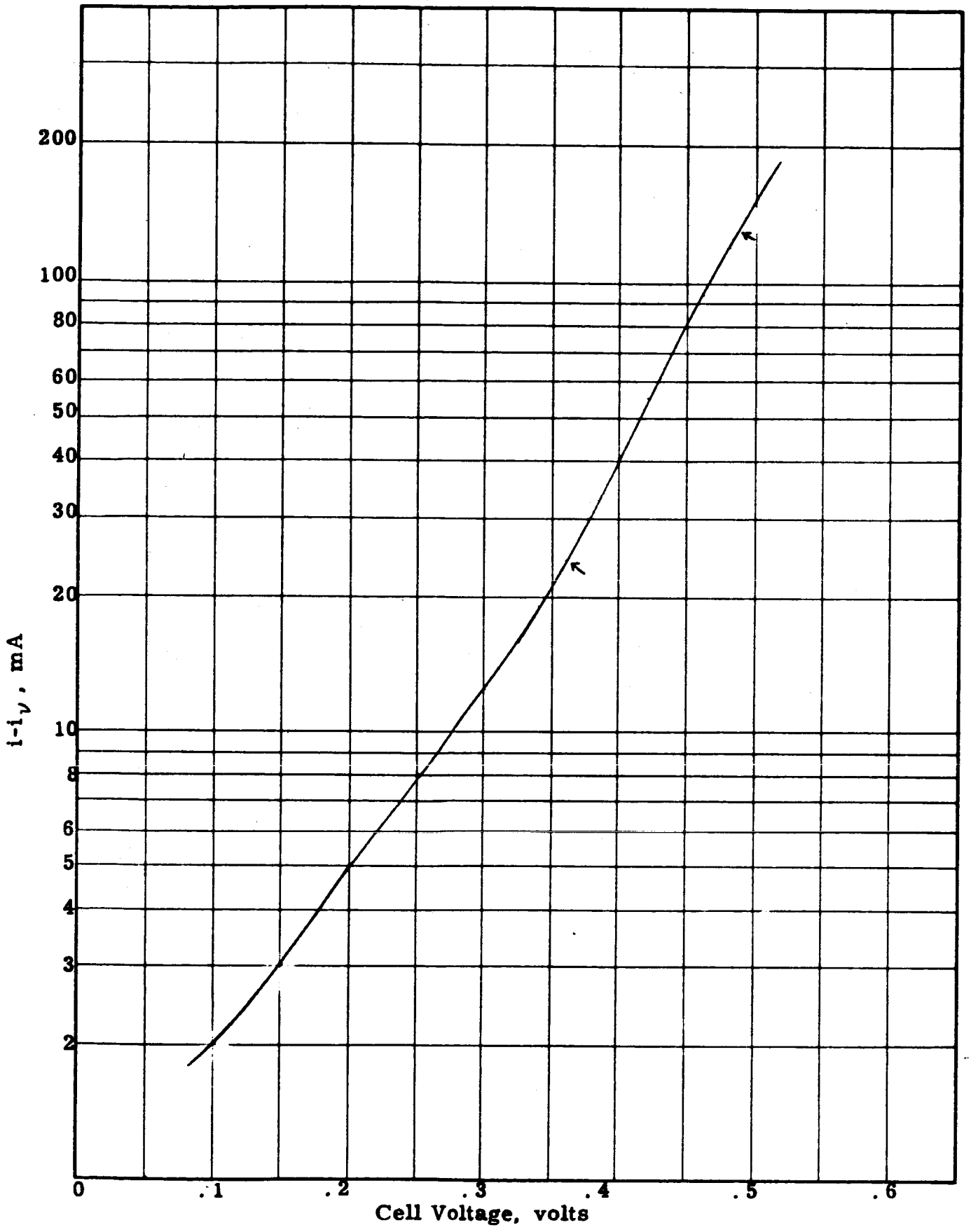

FIG. 4 SEMI-LOG PLOT OF CURRENT-VOLTAGE CHARACTERISTIC OF CdS FILM CELL 160-4.

the computer. These data are plotted in Fig. 5 as the solid curve. The experimentally determined points are also indicated. The agreement appears to be quite good. This is so in the third and fourth quadrants. In the first quadrant, however, there is a significant discrepancy between the theoretical and experimental points, the theoretical points falling below the experimental points. The difference increases with increasing voltage. These differences do not show up when the data are plotted simply because the curve is rising so steeply. This explains the earlier statement that λ, determined by the steepest slope of the semi-log plot, is generally too small for an accurate description of the experimentally determined i-V characteristic in the first quadrant. This raises the question of explaining the good agreement in the third and fourth quadrants.

In order to examine this situation, the computer was programmed to solve Eq. (4-1) with the parameters calculated above and indicated on Fig. 5. The computer was then programmed to solve Eq. (4-1) with $\pm$ 10 percent changes in the parameters i_ν, λ, R_s and R_{sh}. The results are shown in Fig. 6 for $\pm$ 10 percent changes in i_ν and λ. The changes in R_s and R_{sh} were completely insignificant. Changes in i_ν cause major changes in the i-V characteristic: the differences in current being exactly the difference $i \pm \Delta i_\nu$ where Δi_ν is the change in i_ν. Obviously as i approaches Δi_ν the percentage difference can become very large. The changes in λ, however, cause more interesting effects. In the third quadrant, the changes in i are less than 0.5%, much below the limit of detectibility of the measuring equipment. In the fourth quadrant, even the largest differences are only about $\pm$ 4 percent for the $\pm$ 10 percent change in λ. Only in the first quadrant do the differences become really significant; indeed, for the highest voltages the percentage differences may be several times larger than the percentage change in λ.

It is probable that a more correct value of λ can be obtained by using the computer to fit points in the first quadrant. This will yield a value of λ which will be larger than that obtained graphically,

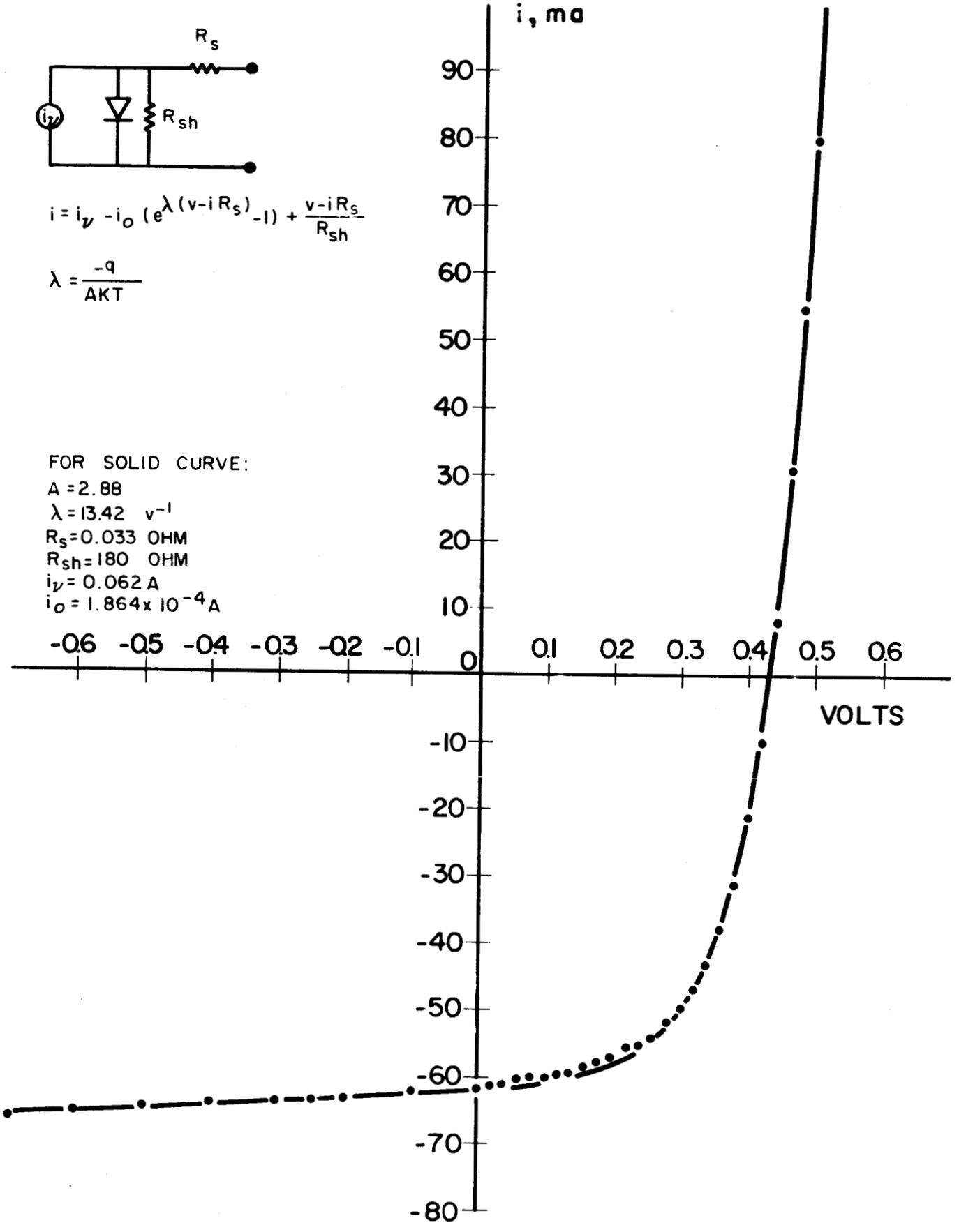

FIG. 5. COMPARISON OF THEORETICAL CURRENT-VOLTAGE CHARACTERISTIC (SOLID CURVE) AND EXPERIMENTAL CURRENT-VOLTAGE CHARACTERISTIC OF CdS FILM CELL 160-4. CELL EFFICIENCY = 2.2 PERCENT.

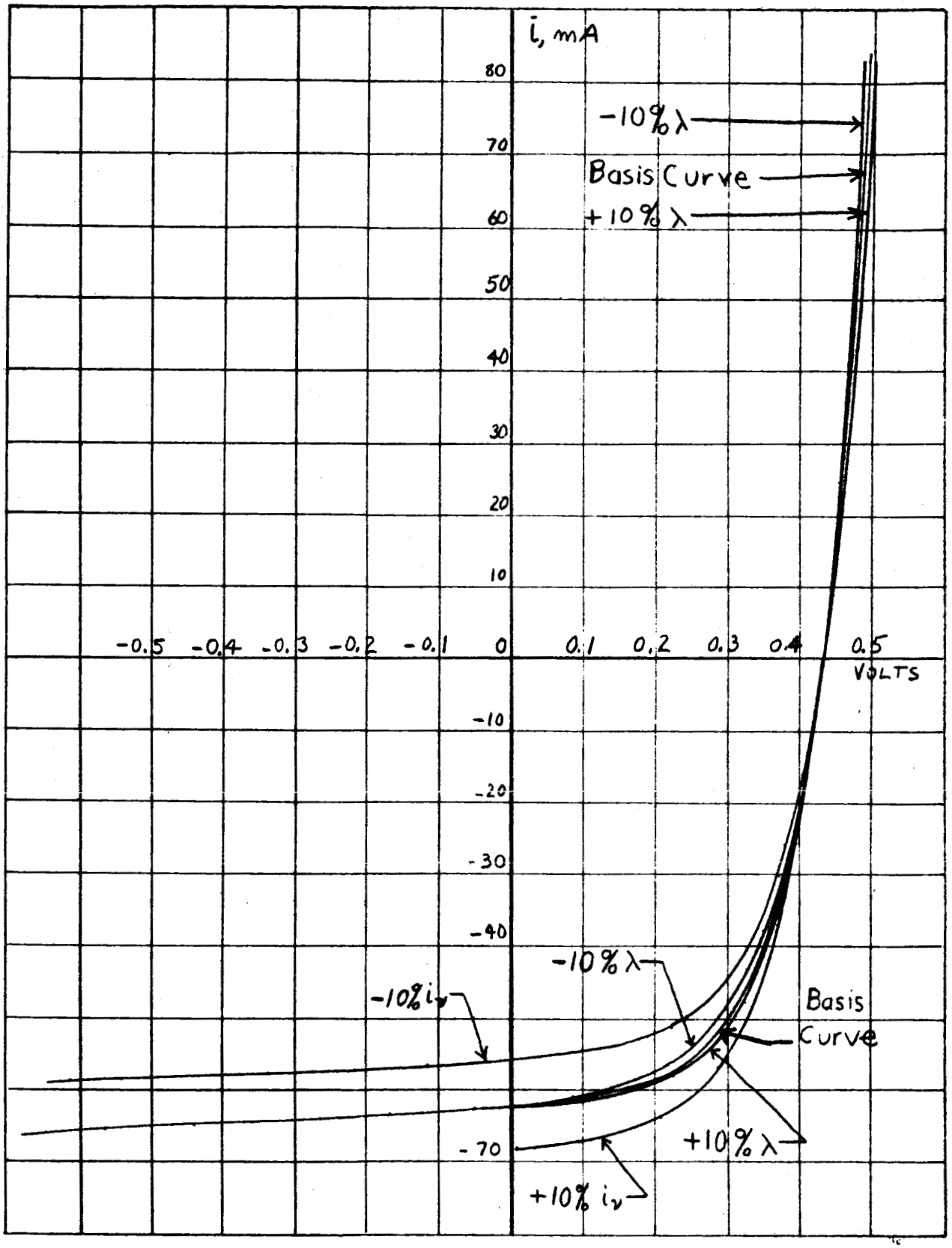

FIG. 6 CURRENT-VOLTAGE CHARACTERISTICS BASED ON CdS FILM CELL 160-4 AND ± 10 PERCENT VARIATIONS IN i_ν AND λ .

but will still permit good agreement in the third and fourth quadrants. This work is yet to be done. Another problem, not yet investigated, is the best way of obtaining i_o and relating it to the fundamental processes taking place in the photovoltaic effect.

5. MISCELLANEOUS

A paper titled "Backwall CdS Film Cells on Plastic Substrates" was presented at the 4th Annual Photovoltaic Specialists Conference at NASA Lewis Research Center, June 2 and 3, 1964.

6. WORK PLANNED FOR NEXT QUARTER

Nearly the entire effort will be devoted to the solution of the CdS-H-Film curling problem. Very promising results have been obtained so far. It is planned to produce several square feet of working cells on H-Film, with the expectation that these cells will exhibit a minimum of curling.

7. REFERENCES

1. W. J. Deshotels, F. Augustine and J. Koenig, "Study of Thin Film Large Area Photovoltaic Solar Energy Converter," Second Quarterly Report, April 17, 1964, Contract No. NAS3-2795, p. 23.

2. W. Shockley, G. L. Pearson, and M. Sparks, Phys. Rev., 76, 180, (1949).

3. C. Sah, R. N. Noyce, and W. Shockley, Proc. IRE, 45, 1228, (1957).

4. H. J. Queisser, Solid State Electronics, 5, 1, (1962).

5. H. G. Grimmeiss and R. Memming, J. Appl. Phys., 33, 2217, (1962).

8. DISTRIBUTION LIST

Copy No.	
	Electronic Research Division
1.	H. Jaffe
2.	Project Administrator
3.	Patent Department
4-6.	Clevite Library
7-16.	Electronic Research Division F. A. Shirland W. J. Deshotels F. Augustine D. A. Berlincourt A. E. Carlson T. R. Sliker L. R. Shiozawa W. K. Bower J. A. Gould J. R. Hietanen
17.	Dr. Gert Lorenz Intermetall G. m. b. H. Freiburg/Breigau Hans-Bunte-Strasse (19), Germany
18-110.	NASA Distribution List (plus two reproducible copies)

NATIONAL AERONAUTICS AND SPACE ADMINISTRATION
DISTRIBUTION LIST

	Copies
National Aeronautics & Space Administration Washington, D. C. 20546	
Attn: Walter C. Scott/RP	2
Attn: H. B. Finger/RP	1
Attn: Millie Ruda/AFSS-LD	1
National Aeronautics & Space Administration Scientific and Technical Information Facility P. O. Box 5700 Bethesda, Maryland 20546	2 + 1 repro.
National Aeronautics & Space Administration Goddard Space Flight Center Greenbelt, Maryland 20771	
Attn: W. R. Cherry	1
Attn: M. Schach	1
Attn: B. Mermelstein, Code 672	1
Attn: J. W. Callaghan, Code 621	1
Attn: Librarian	1
Attn: P. H. Fang, Code 633	5
National Aeronautics & Space Administration Lewis Research Center 21000 Brookpark Road Cleveland, Ohio 44135	
Attn: John E. Dilley, MS 86-1	1
Attn: B. Lubarsky, MS 86-1	1
Attn: H. Shumaker, MS 86-1	1
Attn: R. L. Cummings, MS 86-1	1
Attn: C. K. Swartz, MS 86-1	1
Attn: N. D. Sanders, MS 302-1	1
Attn: Dr. A. E. Potter, MS 302-1	3
Attn: C. S. Corcoran, MS 100-1	1
Attn: N. T. Musial, MS 77-1	1
Attn: George Mandel, MS 5-5	1
Attn: A. B. Smith, MS 49-2	1
Attn: L. R. Scudder, MS 500-201	3 + 1 repro.
National Aeronautics & Space Administration Langley Research Center Langley Station Hampton, Virginia 23365	
Attn: W. C. Hulton	1
Attn: E. Rind	1

	Copies
Jet Propulsion Laboratory 4800 Oak Grove Drive Pasadena, California 91103	
Attn: P. Goldsmith	1
Attn: G. E. Sweetnam	1
Institute for Defense Analysis Connecticut Avenue, N. W. Washington, D. C. 20546	
Attn: R. Hamilton	1
Advanced Research Projects Agency Department of Defense, Pentagon Washington, D. C. 20546	
Attn: Dr. C. Yost	1
Naval Research Laboratory Department of the Navy Washington, D. C. 20546	
Attn: E. Broncato, Code 6464	1
Attn: M. Wotaw, Code 5170	1
Attn: Dr. V. Linnenbom, Code 7450	1
Attn: Dr. C. Klick, Code 6440	1
U. S. Army Advent Management Agency Mission Equipment Department Fort Monmouth, New Jersey	
Attn: William Scherr, SIOFM/PAM-5	1
U. S. Army Signal Research & Development Laboratory Fort Monmouth, New Jersey	
Attn: Power Sources Branch	1
Air Force Cambridge Research Center Air Research & Development Command USAF, Hanscom Field Bedford, Massachusetts	
Attn: Col. G. deGiacomo	1
Air Force Ballistic Missile Division Air Force Unit Post Office Los Angeles 45, California	
Attn: Col. L. Norman, SSEM	1
Attn: Lt. Col. G. Austin, SSZAS	1
Attn: Lt. Col. A. Bush, SSZME	1
Attn: Capt. A. Johnson, SSZDT	1
Attn: Capt. W. Hoover, SSTRE	1

	Copies
Office of the Chief of Engineers Technical Development Branch Washington, D. C. Attn: James E. Melcoln/ENGMC-ED	1
Aeronautical Research Laboratories Office of Aerospace Research, USAF Wright-Patterson AF Base, Ohio Attn: Mr. D. C. Reynolds, ARX Chief, Solid State Physics Research Lab.	1
Wright Air Development Division Wright-Patterson Air Force Base Dayton, Ohio Attn: P. R. Betheand	1
Attn: Mrs. E. Tarrants/WWRNEM-1	1
Flight Accessories Aeronautics Systems Division Wright-Patterson AFB Dayton, Ohio Attn: Joe Wise/Code APIP-2	1
Attn: James L. Matice, ASRCN-22	1
Aerospace Corporation P. O. Box 95085 Los Angeles 45, California Attn: Dr. G. Hove	1
Attn: Dr. F. Mozer	1
Attn: V. J. Porfune	1
Attn: Dr. I. Spiro	1
Attn: Technical Library Documents Group	1
Battelle Memorial Institute 505 King Avenue Columbus, Ohio Attn: L. W. Aukerman	1
Attn: R. E. Bowman	1
Attn: T. Shielladay	1
Bell & Howell Research Center 360 Sierre Madre Villa Pasadena, California Attn: Alan G. Richards	1
Bell Telephone Laboratories, Inc. Murray Hill New Jersey Attn: W. L. Brown	1
Attn: U. B. Thomas	1

	Copies
The Eagle-Picher Company Chemical & Material Division Miami Research Laboratories 200 Ninth Avenue, N. E. Miami, Oklahoma Attn: John R. Musgrave	1
Harshaw Chemical Company Solid-State Division 2240 Prospect Avenue Cleveland, Ohio 44115 Attn: James C. Schaefer	1
Heliotek Corporation 12500 Gladstone Avenue Sylmar, California Attn: Eugene Ralph	1
Hughes Aircarft Company Aerospace Group, R&D Division Culver City, California Attn: C. A. Escoffery	1
Leesona Moos Laboratories 90-28 Van Wyck Expressway Jamaica 18, New York Attn: Stanley Wallack	1
Material Research Corporation Orangeburg, New York 10962 Attn: Vernon E. Adler	1
Martin Company Orlando, Florida Attn: W. A. Headley, Jr.	1
National Cash Register Company Physical Research Department Dayton 9, Ohio Attn: R. R. Chamberlin	1
North American Aviation, Inc. Autonetics Division Anaheim, California Attn: R. R. August	1
Philco Corporation Blue Bell, Pennsylvania Attn: Mr. A. E. Mace	1

	Copies
Radio Corporation of America RCA Research Laboratories Princeton, New Jersey Attn: P. Rappaport	3
Radio Corporation of America Semiconductor & Materials Division Somerville, New Jersey Attn: Dr. F. L. Vogel	1
Sandia Corporation Albuquerque, New Mexico Attn: F. Smits	1
Sylvania Electronic Products, Incorporated Electron Tube Division Emporium, Pennsylvania Attn: Georgiana Larrabee, Librarian	1
Union Carbide Corporation Parma Research Center Technical Information Services P. O. Box 6116 Cleveland, Ohio 44101	1
Solid-State Electronics Laboratory Stanford Electronics Laboratories Stanford University Stanford, California Attn: Prof. G. L. Pearson	1
Westinghouse Electric Corporation Research & Development Laboratories Churchill Borough, Pennsylvania Attn: H. C. Chang	1
Westinghouse Electric Corporation Semiconductor Division Youngwood, Pennsylvania Attn: Don Gunther	1
Massachusetts Institute of Technology Security Records Office Room 14 - 0641 Cambridge 39, Massachusetts	1